ACS SyntheticBiology

pubs.acs.org/synthbio

Research Article

Yeast Synthetic Minimal Biosensors for Evaluating Protein Production

Kai Peng,[‖] Heinrich Kroukamp,[*,‖] Isak S. Pretorius, and Ian T. Paulsen

Cite This: *ACS Synth. Biol.* 2021, 10, 1640–1650

Read Online

ACCESS | Metrics & More | Article Recommendations | Supporting Information

ABSTRACT: The unfolded protein response (UPR) is a highly conserved cellular response in eukaryotic cells to counteract endoplasmic reticulum (ER) stress, typically triggered by unfolded protein accumulation. In addition to its relevance to human diseases like cancer, the induction of the UPR has a significant impact on the recombinant protein production in eukaryotic cell factories, including the industrial workhorse*Saccharomyces cerevisiae*. Being able to accurately detect and measure this ER stress response in single cells, enables the rapid optimization of protein production conditions and high-throughput strain selection strategies. Current methodologies to monitor the UPR in *S. cerevisiae* are often temporally and spatially removed from the cultivation stage or lack updated systematic evaluation. To this end, we constructed and systematically evaluated a series of high-throughput UPR sensors by different designs, incorporating either yeast native UPR promoters or novel synthetic minimal UPR promoters. The native promoters of *DER1* and *ERO1* were identified to have suitable UPR biosensor properties and served as an expression level guide for orthogonal sensor benchmarking. Our best synthetic minimal sensor is only 98 bp in length, has minimal homology to other native yeast sequences and displayed superior sensor characteristics. The synthetic minimal UPR sensor was able to accurately distinguish between cells expressing different heterologous proteins and between the different secretion levels of the same protein. This work demonstrated the potential of synthetic UPR biosensors as high-throughput tools to predict the protein production capacity of strains, interrogate protein properties hampering their secretion, and guide rational engineering strategies for optimal heterologous protein production.

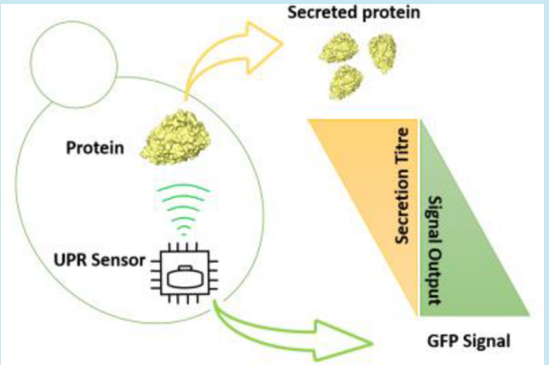

KEYWORDS: *yeast, unfolded protein response, biosensor, synthetic minimal promoter, secretion*

The unfolded protein response (UPR) is a highly conserved cellular response in eukaryotic cells to maintain the endoplasmic reticulum (ER) folding homeostasis and acts as a protective buffer against excessive ER stress.[1,2] When the protein folding workload in the ER exceeds the capacity of its folding machinery, the accumulation of misfolded proteins typically results in the UPR activation. Disruption in the ER membrane morphology or lipid composition has also been shown to trigger the UPR.[3−5] The UPR relieves the ER stress and restores the ER homeostasis by modulating the transcription of UPR-responsive genes (UPR genes)[6] involved in processes to modulate the protein translocation rates in-and-out of the ER, fine-tune the protein chaperone level, expand the volume of the ER, and enhance the ER associated degradation (ERAD) of terminally misfolded proteins.[6−10] The importance of this ER quality control mechanism is highlighted in mammalian cells by the presence of multiple UPR pathways, namely, the PERK, ATF6, and IRE1 pathways, allowing for more precise control of metabolism, translation, and apoptosis to resolve the ER stress.[2,11] The absence or malfunction of the UPR has been linked to various human diseases, including retinitis pigmentosa, multiple myeloma, severe obesity, virus infection, and many types of cancer.[2,5,12]

In the unicellular eukaryote*Saccharomyces cerevisiae*, the UPR pathway is monothreaded, involving two major components: (1) the ER membrane protein Ire1p that acts as the ER stress sensor and signal transducer; and (2) the leucine-zipper transcription activator Hac1p (homologue of the mammalian Xbp1p) as the UPR effector.[13] Hac1p regulates the expression of approximately 400 UPR genes, accounting for approximately 6% of genes in the yeast genome.[6,8] At the onset of ER stress, the Ire1p senses and binds the misfolded proteins *via* its ER luminal misfolded protein binding domain,[14,15] which then triggers the higher-order oligomerization of Ire1p.[16,17] This process is attenuated through the interaction across Ire1p, the

Received: December 17, 2020
Published: June 14, 2021

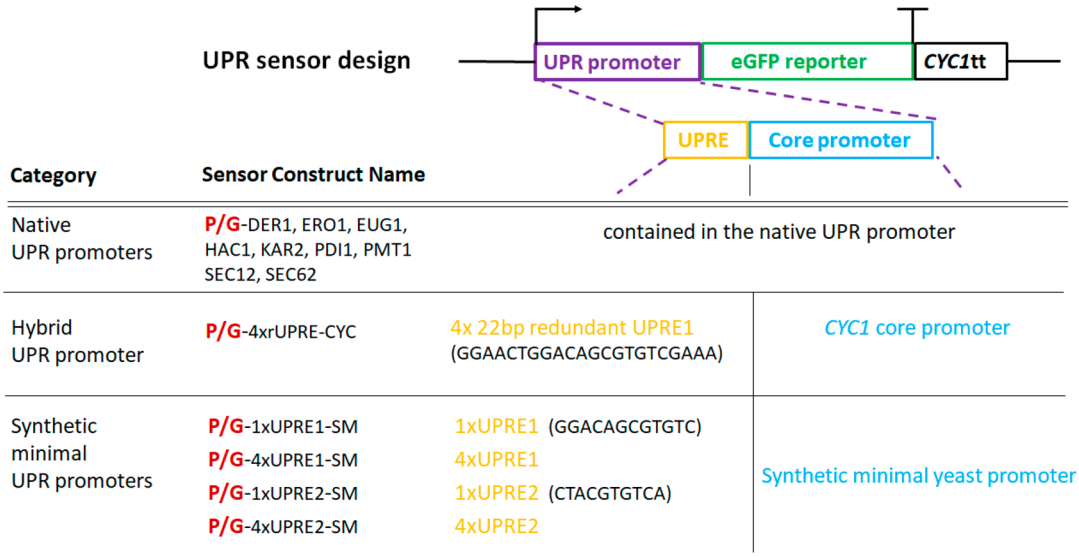

Figure 1. Visual scheme of the UPR sensor design used in this study. Different UPRE and core promoter combinations used for each sensor are indicated. The abbreviated name for each sensor cassette is listed as P, for plasmid form UPR sensor; and G, for chromosome integrated UPR sensor.

essential chaperone Kar2p, and unfolded proteins in the ER lumen.[14] The clustering of Ire1p subsequently activates the RNase activity of its cytosolic domains, allowing for the spliceosome-independent removal of the 252 bp intron from immature *HAC1* mRNA.[13,18] The mature *HAC1* mRNA produced *via* this alternative splicing can be then translated into Hac1p, which subsequently gets imported into the nucleus, where it binds to the upstream activating sequence, called the UPR element (UPRE) to regulate the expression of UPR genes.[13,19−21]

The relatively simple UPR pathway in *S. cerevisiae* has served as a model for elucidating the evolution of the UPR in eukaryotes, the mechanisms of unfolded protein detection, signal transduction, and the transcriptional response, which ultimately restores the ER folding homeostasis. *S. cerevisiae* is also an important cell factory for both recombinant protein and metabolite production,[10,22,23] and engineering strategies often involve the overexpression of native and heterologous proteins, frequently overwhelming the ER's folding capacity and activating the UPR, which has a direct and usually negative impact on the protein production titers. Therefore, in addition to aiding our fundamental understanding of the UPR, the real-time detection and measurement of the UPR in *S. cerevisiae* offers valuable insights into a cell factory's capability to correctly process protein products and allows for the high-throughput optimization of the cultivation and expression strategies.

The conventional methods to detect the UPR induction relied on the detection of the spliced form of *HAC1* mRNA, and an estimate of the activation intensity was determined from the ratio of spliced to unspliced *HAC1* mRNA.[13,24,25] The RNA-based methodologies are time-consuming and susceptible to large technical errors due to the many steps involved. The destructive nature of these methods does not allow for the high-throughput isolation of individual cells of interest. More recently, biological sensors have been developed for mechanistic studies into the UPR regulation. Early sensors exploited the Hac1p-dependent UPRE of the UPR genes, with constructs consisting of one or multiple copies of the 22 bp redundant UPRE consensus sequence 1 (rUPRE1,[19] later refined to the CAGCGTG core sequence[20]), placed upstream of a *CYC1* core promoter, and used enzymatic reporters like *β*-galactosidas,[13,19,26] which are now mostly superseded by fluorescent proteins.[8,27,28] In addition to the UPR transcription mechanism, several UPR sensor designs also tapped into other UPR related non-transcriptional cellular processes as an indirect reflection of the UPR, like using redox-sensitive GFP to detect the redox change in the ER lumen,[27] using fluorescent tagged ER lumen chaperone to monitor its mobility caused by UPR activation,[29] and making an UPR-specific alternative splicing reporter by substituting GFP for the first exon of the *HAC1* gene, which only produces GFP when the alternative splicing occurs.[30]

The previous UPR transcription-based sensors have relied either upon the 22 bp redundant UPRE plus native non-UPR promoter like *CYC1* or upon limited choices of native UPR promoters like those of *HAC1*, *KAR2*,[31] and *ERO1*,[26,32] which could be subjected to additional non-UPR-specific regulation, while in the past decade substantial advances have been made in both UPRE and synthetic minimal promoters in *S. cerevisiae*. In the work by Fordyce et al. in 2012, the authors used systematically designed DNA fragments to investigate their affinity to the Hac1p binding *in vitro* and were able to subsequently refine the previously reported Hac1p binding site to a concise 12 bp core UPRE1 (represented by GGACAG-CGTGTC, UPRE1 hereafter) and 10 bp core UPRE2 (represented by CTACGTGTCA, UPRE2 hereafter). This resolved some of the ambiguity that remained about the prevalence of UPREs in UPR-responsive genes, where it was previously thought that fewer than half of all the UPR genes contained UPRE.[8,26] The harmonization of UPRE also absorbed the previously termed UPRE3[26] into the new framework. Similarly, the refinement of functional core promoters has been reported in *S. cerevisiae*, demonstrating a low but constitutive expression of genes from promoters of merely about 100 bp. These synthetic minimal promoters can be easily converted into stronger inducible promoters through the incorporation of upstream activation sequences (UAS).[33]

https://doi.org/10.1021/acssynbio.0c00633
ACS Synth. Biol. 2021, 10, 1640−1650

These recent developments have prompted the synthetic minimal UPR sensor design described in this study, upgrading the redundant UPRE and the native *CYC1* core promoter in the conventional design into concise UPRE and synthetic minimal core promoter, respectively. Four synthetic minimal UPR sensors were designed, characterized, and systematically evaluated against sensors employing native and hybrid UPR promoters. We selected the G-1xUPRE1-SM sensor as the construct displaying superior resolution, dynamic range, and signal intensity. Furthermore, we showed that this synthetic minimal UPR biosensor could be used to distinguish between cells with different heterologous protein secretion levels, emphasizing its potential as a qualitative high-throughput screening tool to determine the optimal expression and engineering strategies for producing secretory heterologous proteins.

RESULTS AND DISCUSSION

Characterization of Native UPR Gene Expression Profiles. We first investigated the potential of native promoters as effective synthetic parts in building UPR sensors while establishing a more holistic view of the expression characteristics of the native UPR genes in *S. cerevisiae*. Except for some commonly used UPR genes like *KAR2*, *ERO1*, and *HAC1*,[26,31,32] the transcriptional activation profiles of many native UPR promoters have not been documented. To this end, we selected and characterized the expression profiles of nine putative promoters of known UPR genes in *S. cerevisiae*,[8] covering different functional categories of the secretory pathway: *DER1* for misfolded protein degradation, *ERO1*, *EUG1*, *KAR2*, and *PDI1* for polypeptide folding, *PMT1* for protein modification, *SEC12* and *SEC62* for protein trafficking, plus *HAC1* the UPR effector. As UPR genes, their promoters were expected to contain UPRE sequences, the upstream of a functional core promoter. In addition to the known UPREs of *KAR2* and *ERO1*, the putative UPREs of the other genes were predicted on the basis of sequence similarity using Geneious bioinformatics software (Biomatters Ltd.), and these are listed in Table S1. These promoters were cloned to express an eGFP reporter protein to produce the native UPR promoter sensor constructs (Figure 1).

The cells containing the UPR biosensors incorporating the above native UPR promoters were challenged by increasing the concentrations of tunicamycin (Tm), representing the increasing ER stress levels. Tunicamycin is a commonly used UPR chemical inducer and promotes the aberrant folding of proteins by inhibiting the N-linked glycosylation of newly synthesized polypeptides within the ER lumen.[8] Using the eGFP fluorescence output of each sensor construct, we evaluated its ability to resolve differences in Tm concentrations (resolution), the ratio between its maximal and basal response signals (dynamic range), and its absolute fluorescence level (AFU) or signal intensity.

All the nine constructs (indicated by "P-" and the relevant promoter name) had higher unchallenged fluorescence levels ([Tm] = 0 μg/mL) than the control strain harboring a UPR-unresponsive *GAL1* promoter sensor (P-GAL1), indicating the basal level expression in the absence of ER stress (Figure 2). This basal expression of UPR genes was expected since the respective gene products are parts of the native (unstressed) protein processing and recycling pathways. Among all the constructs, the P-ERO1, P-HAC1, P-KAR2, and P-PDI1 sensors had relatively higher basal expression levels (subsequently referred to as the high-AFU group, Figure 2a), with P-KAR2 being the strongest, showing over 65-fold increased AFU compared to that of P-GAL1, while the basal level expressions from P-DER1, P-EUG1, P-PMT1, P-SEC12, and P-SEC62 were significantly lower (the low-AFU group, Figure 2b), ranging from 2- to 10 -fold that of the P-GAL1. When induced, the signals of all nine constructs increased with a rise in the Tm concentration. The P-DER1, P-ERO1, P-HAC1, and P-SEC12 sensors had the best sensitivity to low stress, responding to a Tm concentration of 0.2 μg/mL, while the signals of all the constructs plateaued after 1.0 μg/mL Tm (Figure 2). This signal ceiling could signify the maximal response at which the Ire1p-Hac1p mediated UPR signaling pathway has reached saturation in its transcription activation, or alternatively, it could represent an unfolded protein stress level at which the protein synthesis, including the eGFP reporter itself, is inhibited.

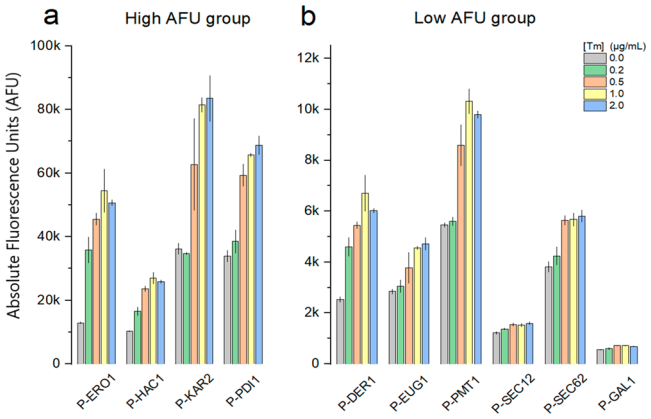

Figure 2. Native UPR promoter sensor response to chemically induced ER stress. The sensor's absolute GFP fluorescence values (AFUs) were divided into (a) high- and (b) low-fluorescence groups. Cells were incubated in tunicamycin concentration gradients for 4 h. Each sample was analyzed as biological triplicates. The *GAL1* promoter construct (P-GAL1) was used as a non-UPR control.

For constructs with AFUs in the lower range, P-DER1 had the best working range and the biggest dynamic range, resolving 0, 0.2, 0.5, and 1.0 μg/mL Tm and reaching a maximal signal of 2.6 times over its basal level. In the high-AFU group, P-ERO1 had the best dynamic range of 4.2 times and, along with the P-HAC1 sensor, had achieved the same resolution as P-DER1. Although P-HAC1 shared these favorable characteristics of P-ERO1 when evaluated under Tm stress, it was unable to separate stress induced by dithiothreitol (DTT) at 2 and 3 mM (Figure S1), which is another commonly used UPR inducer. Considering the best resolution and dynamic range in the low- and high-AFU groups, we selected P-DER1 and P-ERO1 as the most suitable representative native-promoter UPR sensors for benchmarking purposes.

Construction and Evaluation of Synthetic Minimal UPR Sensors. In the current era of synthetic biology, researchers seek to extract genetic components into modular building blocks to make synthetic functional parts or circuits. This ideology, together with the latest developments in *S. cerevisiae* UPRE refinement[21] and synthetic minimal promoter[33] inspired the design of the synthetic minimal UPR sensors described here. In addition to a more concise design embracing "nucleotide economics", another key consideration was to limit the amount of native DNA sequences to improve

https://doi.org/10.1021/acssynbio.0c00633
ACS Synth. Biol. 2021, 10, 1640−1650

the long-term stability of the construct and reduce potential unwanted activation by a cryptic transcription activation sequence. To this end, four synthetic minimal UPR promoters were constructed, containing one or four copies of concise 12 bp UPRE1 (GGACAGCGTGTC) or 10 bp UPRE2 (CTA-CGTGTCA) upstream of a synthetic minimal core promoter (Table S2). Like the native biosensor cassettes, these synthetic minimal UPR promoters drove the expression of eGFP as a reporter (Figure 1). Previous studies have used a native constitutive core promoter *CYC1* with four copies of the 22 bp redundant UPRE placed upstream.[27,34] We referred to it as the "hybrid" UPR sensor in this study (Figure 1) in order to differentiate our constructs from chemically synthesized promoters based on yeast native sequences, which in the past were often referred to as "synthetic promoters". Thus, the synthetic minimal UPR sensor design had a more concise UPRE and a fully synthetic core promoter design, in contrast to the redundant UPREs and the native *CYC1* core promoter in the conventional hybrid sensor. We then compared the UPR stress response characteristics of each UPR promoter category, namely, the native UPR promoters, the hybrid UPR promoter, and the synthetic minimal UPR promoter, in order to determine the ability of each to report on UPR. All these sensors were chromosomally integrated as a single copy at the *flo8* locus. This was done to achieve the enhanced homogeneity (reduced noise) of a single cell fluorescence signal within the population (Figure S2), due to reduced construct copy number variability and enhanced construct stability. We repeated the Tm gradient stress test for these constructs and evaluated the sensor response on the basis of the criteria of resolution and dynamic range as the previous section. Because the excessive eGFP synthesis itself may exert stress or compete for the protein processing machinery, especially relevant in cell factories producing heterologous proteins, the signal intensity (AFU) was also considered as an evaluation criterion.

The G-DER1 and G-1xUPRE2-SM sensors were the only ones able to significantly resolve the UPR induction difference between the unstressed state and a Tm concentration of 0.1 μg/mL ($p < 0.05$) (Figure 3a). Since both *DER1* and *ERO1* promoters were selected on the basis of their ability to previously display significant activation at 0.2 μg/mL Tm; this lower stress level may signify the turning point where significant unfolded protein stress had accumulated to initiate the UPR. Except for G-ERO1 and G-4xUPRE1-SM, all sensors could distinguish between 0.1, 0.3, 0.5, and 0.75 μg/mL Tm ($p < 0.05$) (Figure 3). At higher stress levels, only the synthetic minimal sensors G-1xUPRE1-SM, G-4xUPRE1-SM, and G-4xUPRE2-SM successfully resolved 0.75 from 1.0 μg/mL ($p < 0.05$). The different capacities of resolving high ER stress (Tm = 0.75−1.0 μg/mL) between the constructs indicated the different transcriptional behavior between the UPR promoter designs, instead of the UPR signaling pathway being "saturated" by the ER stress at this level. Therefore, G-1xUPRE1-SM and G-4xUPRE2-SM had the widest working range across all the constructs, performing well between 0.1 and 1.0 μg/mL Tm. Although the hybrid sensor G-4xrUPRE-CYC had distinct separation covering Tm concentrations of 0.1−0.75 μg/mL, it lacked sensitivity at both the lower and higher stress levels (Figure 3b).

For single cell application, sensors are subjected to the inherent stochastic biological variability among cells, thus sensors with a large signal dynamic range are highly desired.

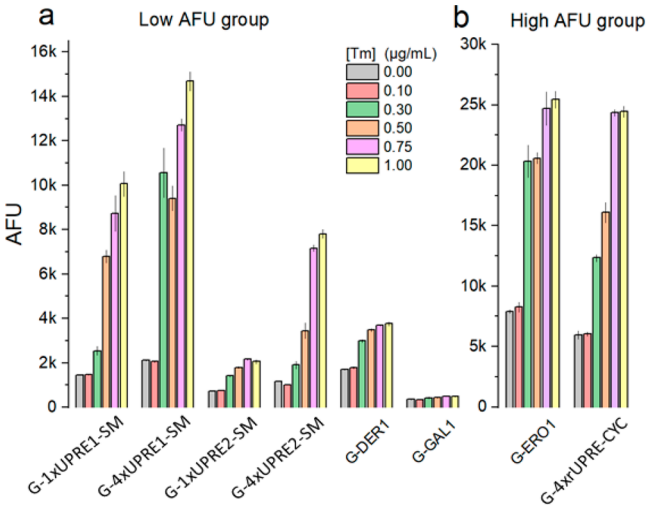

Figure 3. Synthetic minimal UPR sensor (G-1/4xUPRE1/2-SM) response to chemically induced ER stress. A conventional hybrid (G-4xrUPRE-CYC) sensor and *DER1* and *ERO1* (G-DER1/ERO1) promoter sensors were also evaluated. The sensors were divided into the (a) low- and (b) high-AFU groups for display. Cells were incubated in tunicamycin concentration gradients for 6 h. Each point represents at least three biological replicates. The *GAL1* promoter construct (G-GAL1) was used as a non-UPR control.

Here again, the G-1xUPRE1-SM, G-4xUPRE1-SM, and G-4xUPRE2-SM sensors had the largest dynamic ranges ∼7-fold those of their respective uninduced signal levels (Figure 3). Although G-DER1 was sensitive to 0.1 μg/mL Tm, it had the lowest dynamic range of all the evaluated sensors, only managing ∼2-fold over its basal level. Overall, the G-1xUPRE1-SM and G-4xUPRE2-SM synthetic minimal UPR sensors had the best dynamic signal and working ranges. They also had intermediate signal strength throughout the working ranges, reducing concerns about the influence of eGFP production. Producing excessive GFP as a signal output, like G-ERO1 and G-4xrUPRE-CYC, may exert stress and compete for the cellular resources, which is especially relevant to cells producing recombinant protein. On the contrary, having too weak a signal like G-1xUPRE2-SM might cause difficulty in determining if UPR is activated and obscure the difference in signals. UPRE2 elicited a weaker transcriptional activation than UPRE1, and even with four copies, G-4xUPRE2-SM only had ∼80% the signal strength of G-1xUPRE1-SM with a single copy of UPRE1. In addition to the functional advantages of the synthetic minimal UPR promoters G-1xUPRE1-SM and G-4xUPRE2-SM, they are substantially smaller than the 383 bp hybrid sensor, with 98 and 126 base pairs, respectively. The G-1xUPRE1-SM sensor was selected for subsequent experiments, due to its more compact design and the theorized reduced probability of containing off-target regulatory elements.

Evaluation of *HAC1*-Independent Biosensor Noise. Besides the resolution, dynamic range, and signal intensity criteria, we were also interested in determining whether the biosensor exclusively responds to Hac1p-dependent transcriptional activation in our cultivation conditions. Complete orthogonality is not always achievable in biological systems, considering the complex and interconnected nature of cellular metabolism. However, with careful biosensor design and by limiting the promoter size, we aimed to minimize any indirect off-target response or noise. For example, it has been shown that the UPR gene *KAR2* has a functional heat shock response

https://doi.org/10.1021/acssynbio.0c00633
ACS Synth. Biol. 2021, 10, 1640−1650

element,[19] and repeats of the heat shock motive, nGAAn, were found in the UAS region of the 4xrUPRE-CYC construct. While our bioinformatics analysis of the synthetic minimal promoter constructs did not reveal any known stress-responsive UAS element other than the UPRE, we also wanted to assess whether the signal levels were influenced by transient Hac1p transcription factor levels under unstressed conditions. Since Hac1p is known to be the sole activator of UPR in *S. cerevisiae*, we evaluated the Hac1p-dependent and Hac1p-independent response of the UPR sensors in the wild type and *hac1* deleted strains to compare the signal-to-noise ratios of different constructs (Figure 4). The P-DER1, P-ERO1, P-4xrUPRE-CYC, P-1xUPRE1-SM, and P-4xUPRE2-SM constructs were chosen to represent the native, hybrid, and synthetic minimal UPR sensor categories.

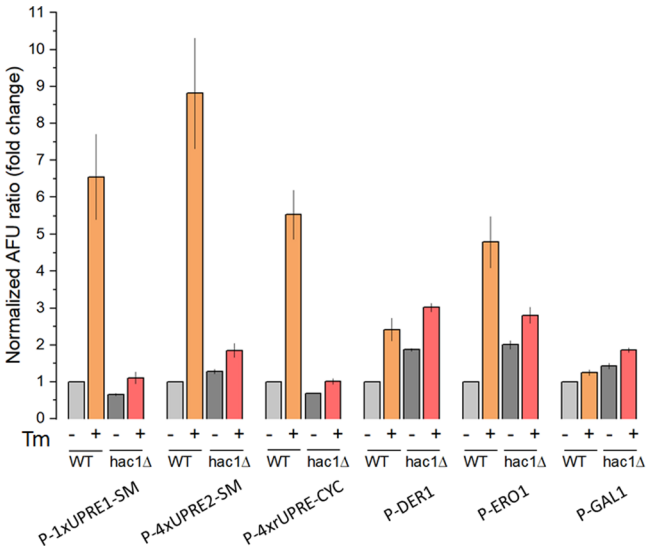

Figure 4. Response of UPR sensors in wild type (WT) and *hac1* deleted (*hac1*Δ) strains. The unfolded protein response was evaluated in the presence (+) or absence (−) of 0.5 μg/mL tunicamycin for 6 h. The AFU values were normalized against the untreated WT value of each sensor construct to represent the fold change in response. The *GAL1* promoter construct served as the non-UPR control. The error bars represent the standard deviation of at least three biological replicates.

For all the five UPR sensors, unstressed basal-level fluorescence was observed in both *hac1*Δ and wild type strains over the P-GAL1 control. To normalize across the different basal levels of signal in wild type and *hac1*Δ strains, the response to Tm was presented as the fold change in signal when induced over the basal level of the relevant wild type or *hac1*Δ strain. By measuring the Hac1p-independent residual response (relative response in *hac1*Δ versus WT strain), we were able to detect other contributions to sensor activation, which was not due to Hac1p binding and thus an indication of sensor orthogonality under URP stress conditions: the smaller the Hac1p-independent residual response, the better the orthogonality. As expected, the response of all the sensor constructs was significantly suppressed in *hac1*Δ strains when compared to that of the corresponding wild type under UPR stress conditions (Figure 4). While there was no significant difference between the hybrid P-4xrUPRE-CYC and P-1xUPRE1-SM, the P-4xUPRE2-SM sensor achieved a significantly lower residual response than the other two ($p <$ 0.05), merely 16% of the full response in wild type. In the native UPR promoter group, the P-ERO1 sensor managed to rival P-4xrUPRE-CYC and P-1xUPRE1-SM by having a similar residual response around 26−29%, while the P-DER1 still retained a 67% response to Tm even without the UPR pathway, which might echo the function of Der1p as an ERAD pathway component. The activation of the native sensors in the *hac1*Δ strain, when not subjected to Tm stress, was unexpected but demonstrates inherent safety circuitry (or evolutionary redundancy) within biological systems to protect itself. This complex behavior of the native UPR promoters makes them less suitable for the sensitive detection of the UPR. In contrast, the synthetic minimal design is not only more concise but also incorporates better characterized DNA sequences to enhance the specificity in response and minimize off-target effects, thus advantageous over arbitrary native genetic parts.

Detecting ER Stress Caused by Misfolded Proteins. *S. cerevisiae* not only serves as a model organism to study the mechanism of the UPR but also is a persistent organism of choice as a cell factory for heterologous protein. It has been frequently noted that the overproduction of protein can activate the UPR by overwhelming the protein folding capacity and subsequently lead to higher rates of protein aggregation and degradation. This implies that the standard methods of boosting protein production, such as increasing the copy number of genes of interest, and the use of strong promoters to drive expression could ultimately trigger the UPR. Although the initial increased ER folding capacity brought in by the UPR may benefit some protein products, continuous high-level UPR activation generally results in a negative net impact on the secretion titers.[35] For this reason, a quantitative evaluation and early detection system of ER stress in protein producing cell factories is of great importance and, in addition, could serve as a high-throughput tool to understand the strain-dependent or protein-specific factors contributing to UPR induction.

To this end, we evaluated our synthetic minimal sensor's ability to resolve ER stress caused by protein production. We overexpressed the *S. cerevisiae* carboxypeptidase Y (CPY) and its mutated version (CPY*) in our G-1xUPRE1-SM biosensor strain. CPY is a native vacuolar peptidase, while the mutant form CPY* has a single amino acid mutation of G255R, which makes it prone to aberrant folding and aggregation in the ER lumen. CPY* expression is frequently used as a model system to stimulate UPR activation in yeast.[27,36] To create differentiated protein expression levels, low (centromeric pRS413 vector) and high copy number vectors (2 μ pRS423 vector) were used to drive the expression of CPY and CPY*. After 12 h of incubation, the overexpression of wild type CPY from low and high copy vectors elicited unfolded protein responses of ∼2.5-fold and ∼3.1-fold over the basal level at time point zero, respectively (Figure 5). When considering the minimal responses from the empty vectors, it was clear that the UPR was induced by the misfolding of the native protein and that the overexpression of some native proteins itself could cause significant ER stress, a consequence that should be taken into account when modulating native host pathways like promoter exchange. For the mutated CPY* strains, significant increases in sensor signal were observed for both the low and high copy strains, with ∼3.4- and ∼5.1-times of the basal level signal at 12 h (Figure 5). These findings aligned with previous studies, where the UPR effect of protein production is caused by both the difficulty of polypeptide folding and the protein workload.

https://doi.org/10.1021/acssynbio.0c00633
ACS Synth. Biol. 2021, 10, 1640−1650

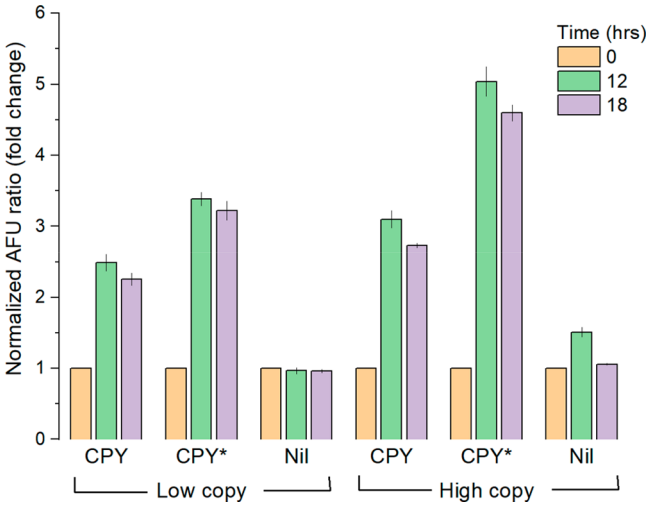

Figure 5. G-1xUPRE1-SM UPR sensor response in strains producing native CPY and its perpetually misfolded form CPY* on low and high copy number expression vectors. GFP signal was measured at 0, 12, and 18 h after inducing expression with galactose. Strains containing empty versions of the low or high copy vectors (Nil) were used as controls. The AFU values from the sensors were normalized against the time point zero value of each sample, to represent the fold change in response. The error bars represent the standard deviation from at least three biological replicates.

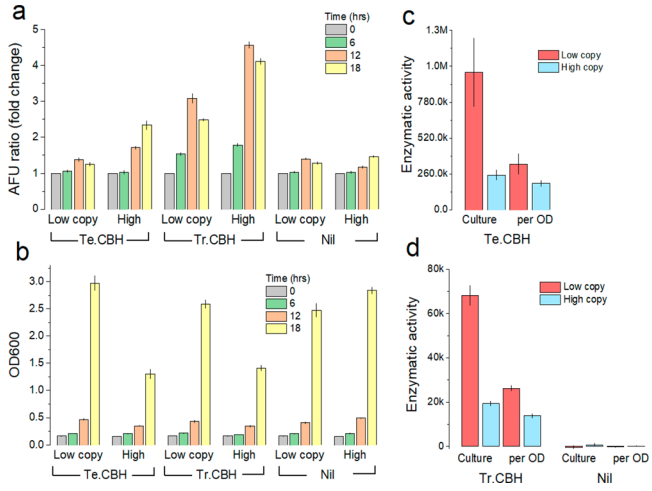

Figure 6. G-1xUPRE1-SM UPR sensor response to recombinant protein production stress. (a) G-1xUPRE1-SM UPR sensor response in strains producing Te.CBH and Tr.CBH *via* low and high copy expression vectors. The expression of CBH was induced using 2% galactose, and the AFU was measured at 0, 6, 12, and 18 h. Strains with empty vectors (Nil) were used as a control. The AFU was normalized against the time point zero value of each sample to represent the fold change in signal. (b). Cell density (OD_{600}) of the above strains at different time points after induction. (c and d) Enzymatic activity of Te.CBH, Tr.CBH, and an empty vector control measured through MULac assay after 18 h of induction. To compare the CBH secretion at a per cell level, the enzymatic activity readings from the supernatant of relevant strains (Culture) were also normalized against the OD_{600} (per OD). The error bars represent the sample standard deviation from at least three biological replicates.

It thus verified the G-1xUPRE1-SM sensor's ability to detect the difference in ER stress generated by both situations.

Rapid Evaluation of Expression Strategies on Heterologous Protein Expression. One of the key benefits of using yeast as a cell factory is its ability to efficiently secrete proteins into the environment. We have demonstrated the capacity of our G-1xUPRE1-SM sensor to differentiate between native and aberrantly folded protein, which only partially completes the journey to the cell membrane. In a study by Ilmén et al. in 2011, it was observed that, out of 14 evaluated cellobiohydrolase I (CBH) enzymes expressed in yeast, the *Trichoderma reesei* Cel7A (Tr.CBH) and the *Talaromyces emersonii* Cel7A (Te.CBH) had the lowest and highest active secreted enzyme yields, respectively. To evaluate the sensor's capacity to detect potential UPR induction in strains producing commercially valuable secretory proteins and whether differences in UPR can be detected between different recombinant proteins and production loads, we studied the G-1xUPRE1-SM sensor response in strain expressing Te.CBH and Tr.CBH *via* low and high copy vectors, as in the previous section. The presence of Te.CBH and Tr.CBH secreted was also verified by targeted proteomics (Figure S3).

Six hours after inducing the CBH expression, significant increases in signals ∼1.5- and ∼1.8-fold that at T_0 became observable in strains expressing Tr.CBH on low and high copy vectors, respectively (Figure 6a). This ER stress was detected prior to any Tr.CBH activity that could be measured in the supernatant (data not shown). For Te.CBH, such early stimulation of the UPR was undetectable by 6 h. But at 12 and 18 h, all strains except the low copy Te.CBH had increased signals. At 12 h after induction, the low and high copy Tr.CBH strains had more than triple the signal, reaching ∼3.1 and ∼4.6 times their uninduced levels. Like the CPY* experiment, the high copy Tr.CBH induced a significantly stronger signal than the low copy, showing increasing protein workload that further aggravated the ER stress. By 18 h, the signal intensity dropped to around ∼2.5 and ∼4.1 times the basal level, which might reflect the cellular effort to re-establish the equilibrium between the protein folding capacity and the protein workload. On the contrary, both the low and high copy Te.CBH strains showed significantly lower UPR induction than the corresponding Tr.CBH strains ($p < 0.05$), with 0.4-fold and 0.7-fold increase over their basal level signal by 12 h (Figure 6a). Our UPR biosensor results were consistent with the findings by Ilmén et al. in 2011, who observed significantly higher levels of spliced *HAC1* mRNA, thus the UPR magnitude, in strains expressing the Tr.CBH than Te.CBH.

The production of various heterologous proteins and the expression strategy of choice affect not only the UPR level but also the cell growth as well. The two high copy CBH vector strains reached a similar optical density (OD_{600}) after 18 h. But, unlike the low copy versions, they had significantly impacted cell growth, only reaching around 55% that of the low copy control strain (Figure 6b). Lowered biomass yield is not uncommon in yeast strains overproducing heterologous proteins[37] and has been reported for Te.CBH expressed from a high copy vector.[38] Similar reductions in biomass have previously been reported as a direct result of constitutive UPR induction,[39] while others suggested that this is a consequence of the increased metabolic burden exerted by high levels of protein synthesis.[35] Our results supported the latter observation, since the cell densities of Te and Tr.CBH high copy strains were similarly low by 18 h, regardless of the significant difference in the UPR signal. This also suggested that the change in cell biomass is not a suitable proxy to infer general protein production levels nor an indication of the UPR induction level.

https://doi.org/10.1021/acssynbio.0c00633
ACS Synth. Biol. 2021, 10, 1640−1650

Concomitant with the lower UPR level, the low copy Te.CBH and Tr.CBH expressing strains both achieved over 3 times CBH activity in culture than their high copy counterparts (Figure 6c,d). Because the enzymatic activity in culture is a function of both the secretion at a per cell level and the number of cells in the culture, we normalized the culture enzymatic activity against the cell density (OD_{600}) to represent the secretion at a cellular level, consistent with the sensor signal. The correlation between a greater UPR and a concomitant lowered protein secretion was valid at both culture and per cell levels (Figure 6c,d). Therefore, the higher secretion titer from low copy Te.CBH and Tr.CBH was not merely a function of faster cell growth or density but also a result of higher secretion at a cellular level. Since it is known that increases in the gene copy number do not have a linear correlation with protein production levels and could even be detrimental to the overall protein yield, the ability of our G-1xUPRE1-SM sensor to report on the relationship between the UPR levels induced by different copies of CBH and the concomitant protein titers highlights its application in optimal gene copy number determination. Our findings also demonstrated the application of our UPR biosensor as an early indicator of the UPR, even before the protein of interest is detectable by conventional methods. Since the UPR directly impacts protein production, this novel screening tool has the potential to maximize the protein yield at an early stage of strain development. In addition, the UPR-sensor-based assay is fast, inexpensive, and allows for high-throughput screening with fluorescence activated cell sorting, without requiring a destructive protocol or harsh chemical treatment, which could be detrimental to other downstream analysis like enzymatic- or antibody-dependent assay.

Rapid Evaluation of Host Strain Secretory Capacity. We have so far shown that our biosensor is capable of distinguishing between high and low protein production levels conferred by different vector systems. In addition to the expression strategy, protein production is also highly dependent on the genetic background of the host strain used, and big differences in secretion capacity exist even between commonly used laboratory strains.[38] The genetic makeup of a strain could directly impact its secretion capacity through factors like changes in the secretory pathway componentry[40] or indirectly by culturing conditions such as heat or nutrient stress. In addition, protein yields are often highly protein specific[41] and often require a low-throughput expression characterization of samples to reliably identify the desired protein/strain candidates. Considering the significant impact UPR has on protein production and how the strain's genetic background can modulate this response, we set out to determine whether an elevated UPR would cause a diminished secretory protein yield in *S. cerevisiae* from a different strain lineage, as observed in our low/high protein expression experiment.

Therefore, we investigated how the commonly used *S. cerevisiae* strain CEN.PK2-1C performed when challenged with protein production stress. Since Tr.CBH elicited a stronger UPR response in our previous experiment, we introduced the G-1xUPRE1-SM biosensor and low copy Tr.CBH expression vector into the CEN.PK2-1C strain and evaluated its respective secretion capacity and UPR activation, relative to those of the BY4742 strain. After 12 h of incubation, the G-1xUPRE1-SM sensor response rose to around 3 times the basal level (T_0) in the BY4742 strain, consistent with our previous result (Figure 7a). In sharp contrast, the CEN.PK2-1C strain had a signal

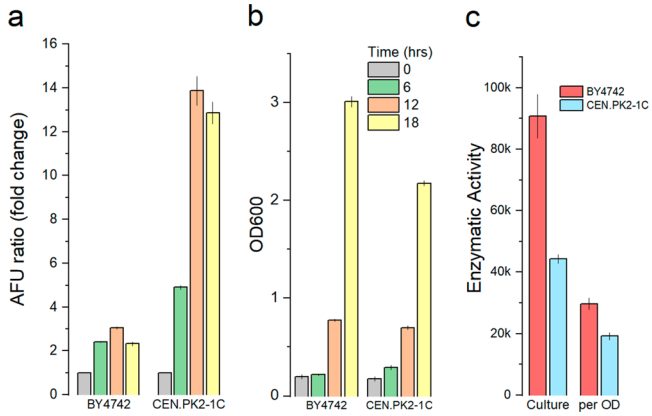

Figure 7. Evaluating protein production stress tolerance in BY4742 and CEN.PK2-1C strains using the G-1xUPRE1-SM UPR sensor. GFP fluorescence measurements for strains expressing Tr.CBH on low copy vectors in BY4742 and CEN.PK2-1C yeast strains. (a) UPR sensor signal was read at 0, 6, 12, and 18 h after inducing the Tr.CBH expression with 2% galactose. The AFU was normalized against the time point zero value of each sample to represent the fold change in response. (b) Cell density (OD_{600}) measured at each time point. (c) Tr.CBH enzymatic activity was compared through MULac assay, as done previously in Figure 6. The error bars represent the sample standard deviation from at least three biological replicates.

increase almost 14-fold over the same growth period (Figure 7a). Although both strains have been established as commonly used lab strains, the significantly stronger UPR activation in the CEN.PK2-1C strain demonstrated the implication of the similar but still heterogeneous genetic background on common stress responses. Interestingly, the CEN.PK2-1C strain grew significantly slower than BY4742 by 18 h (Figure 7b), likely due to the high level of UPR induction. As expected from our previous data, the strong UPR in the CEN.PK2-1C strain was also correlated with a lowered extracellular Tr.CBH yield, with the BY4742 culture having over twice the enzymatic activity of CEN.PK2-1C by 18 h, brought about by a higher per cell level secretion in addition to a faster growth (Figure 7c). This echoed the previous observation that a lower UPR leads to higher secretion and indicated that this UPR/secretion relationship could potentially be exploited using our UPR biosensor to facilitate high-throughput screening to survey the secretion capacities of different *S. cerevisiae* strains.

SUMMARY

The optimal production of recombinant proteins in yeast is dependent on the delicate balance between the protein synthesis load and the ER's ability to effectively process it. This balance is further influenced by factors such as the growth media composition, the biophysical properties of the protein of interest, and the small but significant differences in cellular metabolism between genetically distinct strains. Here, we have constructed and evaluated novel synthetic minimal UPR biosensors with enhanced resolution, dynamic range, and signal intensity. These sensors were modular in design and took advantage of updated genetic information on the regulatory elements of UPR genes and recent advances in synthetic minimal core promoter research. Considering the tremendous impact of the ER's folding capability on the cells' ability to produce and secrete proteins, an early detection and evaluation tool has substantial fundamental and industrial value. Our sensor was able to detect UPR differences caused by

https://doi.org/10.1021/acssynbio.0c00633
ACS Synth. Biol. 2021, 10, 1640−1650

different proteins, abnormalities in protein folding, and expression levels. Although the reasons for many of the highly protein-specific differences in protein production are still unknown, biosensors like the ones described here represent a significant advancement in the detection of a major bottleneck in protein processing and opens the door for high-throughput screening approaches.

METHODS

Media and Growth Conditions. *Escherichia coli* DH5α (deoR endA1 gyrA96 hsdR17 6[lac]U169 recA1 relA1 supE44 thi-1 [q80 lacZ6M15]) was grown in Luria−Bertani broth (10 g/L NaCl, 10 g/L tryptone, and 5 g/L yeast extract) or on Luria−Bertani agar plates supplemented with 100 μg/mL ampicillin to select plasmid-containing cells. *Saccharomyces cerevisiae* strains were routinely cultured in YPD media (20 g/L glucose, 20 g/L peptone, and 10 g/L yeast extract) at 30 °C and 200 rpm shaking for all liquid cultures. Yeast strains containing the native promoter biosensor and hybrid and synthetic minimal biosensor constructs either as plasmids or in genomically integrated form were selected and maintained on SC^{-ura} media (6.7 g/L yeast nitrogen base, 1.9 g/L yeast dropout supplement without uracil, 20 g/L glucose, and 20 g/L bacteriological agar for plates). CPY and CBH expression plasmids were selected and maintained in SC^{-his} media (6.7 g/L yeast nitrogen base, 1.9 g/L yeast dropout supplement without histidine, 20 g/L glucose, and 20 g/L bacteriological agar for plates). Putative *hac1* deletion transformants were selected on YPD agar plates supplemented with 300 μg/mL G418 sulfate. The induction of protein expression in strains harboring the CPY and CBH gene cassettes was achieved by transferring washed SC^{-his} grown cells into $2xSC^{-his}$ (gal) (13.6 g/L yeast nitrogen base, 3.8 g/L yeast dropout supplement without histidine, 20 g/L galactose, 20 g of succinic acid, 12 g of sodium hydroxide, adjusted to pH 6.0).

Plasmid and Recombinant Strain Construction. DNA manipulations were done following standard protocols. All molecular biology reagents and kits were purchased from New England Biolabs and used as directed by the manufacturer unless otherwise stated. The yeast transformation was done using the LiOAc/ssDNA method.[42]

Biosensor Vector and Strain Construction. The scheme of UPR sensor design and the plasmids used in this study are summarized in Figure 1 and Table S3, respectively. The putative promoters of the nine native UPR genes were isolated by PCR from *S. cerevisiae* S288c genomic DNA using the primers described in Table S4, which lists the primers used in this study. For the construction of the native promoter biosensor plasmids, purified promoter PCR amplicons were digested with PacI and *Eco*RI and subsequently cloned into the pRS416-PGK 1p-eGFP-CYC1t plasmid digested with the same restriction enzymes. These biosensor plasmids were designated as pRS416-[promoter name] and were transformed into the *S. cerevisiae* CEN.PK2-1C[43] strain and selected on SC^{-ura} agar plates.

A base integrative vector was constructed, which allowed for the targeted integration of biosensor construct to the neutral *flo8* genomic locus of *S. cerevisiae*. The *flo8* orf was amplified with the FLO8orf-F/R primer set and the amplicon cloned into the pJET1.2/blunt vector using a CloneJET PCR cloning kit (Thermo Scientific). The plasmid backbone and the flanking >200 bp of the flo8 orf were amplified using the FLO8int-F/R primer incorporating NdeI, *Eco*RI, and AfeI restriction sites. pRS416 was digested with *Eco*RI and AfeI to isolate the *URA3*-marker-containing fragment, which was cloned into the corresponding sites of the pJet-Flo8 vector. The *DER1*-biosensor cassette was liberated from the pRS416-DER1 plasmid with *Eco*RI and NdeI and directionally cloned into the corresponding site of the Flo8- and *URA3*-containing cloning vectors to yield G-DER1 construct. G-ERO1 was constructed by isolating the *ERO1* promoter fragment from the pRS416-ERO1 plasmid using *Eco*RI and PacI and replacing the *DER1* promoter in the G-DER1 construct. Synthesized minimal (1/4xUPRE1/2-SM) and hybrid (4xrUPRE-CYC) UPR promoter fragments were inserted into the Flo8- and URA3-containing cloning vectors, using *Eco*RI and PacI the same way as G-ERO1. The nucleotide sequence of the synthetic minimal and hybrid UPR promoters are listed in Table S2. The integrative biosensor cassettes were amplified from their respective plasmids using the FLO8orf-F/R primers, and the PCR products were used to transform *S. cerevisiae* CEN.PK2-1C and BY4742 strains. Putative transformants were selected on SC^{-ura} agar plates, and the successful integration of the cassettes was confirmed with PCR using the FLO8con-F/R primer set.

Protein Production Vector and Strain Construction. The native *CPY1* ORF of *S. cerevisiae* was isolated *via* PCR from the genomic DNA of BY4742.[44] The PCR amplicon was purified and digested with PacI and AscI and cloned into the pRS413/423-GAL-CYC1 plasmids. PCR and GoldenGate assembly (*via* SapI) were used to introduce the G255R mutation into the native CPY to make CPY*. The CPY* fragment was cloned into pRS413/423-GAL-CYC1 vectors the same way as CPY. The Te.CBH ORF was isolated from the pMU(hph)_Te.CBH1 vector,[38] and the Tr.CBH orf was chemically synthesized (IDT).[40] Both fragments were digested and cloned in pRS413/423-GAL-CYC1 as described previously. These plasmids were named using the following convention: pRS413/423-[protein name]. The CPY and CBH expression vectors were individually used to transform strains containing chromosomally G-1xUPRE1-SM biosensor and selected on SC^{-his} agar plates.

Chemical Induction of the UPR Using Tunicamycin. Mid log phase cells were inoculated into buffered double-strength $2xSC^{-ura}$ media (13.6 g/L yeast nitrogen base, 3.8 g/L yeast dropout supplement without uracil, 20 g/L glucose, 20 g/L succinic acid, and 12 g/L sodium hydroxide, adjusted to pH 6.0) to obtain starting optical densities of 0.15 at OD_{600} for native and *hac1* deletion strains with UPR biosensors. Tunicamycin concentrations and sampling times are indicated for each experiment. All tunicamycin stress cultivations were performed at 30 °C with 200 rpm shaking. For the comparative native UPR promoter tests, the cells were grown in triplicate in a 250 mL shake flask with 30 mL of media. All subsequent experiments were done in quadruplicate in 24-well plates sealed with sterile gas-permeable AeraSeal membranes (Sigma-Aldrich, Castle Hill, Australia) with 1 mL of media per well, unless otherwise stated.

Biosensor Fluorescence Detection. At relevant time points, a sample of the yeast culture was taken and loaded into 96-well plates and diluted down to OD_{600} 0.5 if needed. A Beckman Cytoflex S flow cytometer was used to determine the mean GFP fluorescence of the cells, using the default FITC channel (ex/em 488/525 nm) to record 10 000 events. The flow rate was controlled around 100−2000 events/second to ensure single cell readings. Default settings corresponding to

https://doi.org/10.1021/acssynbio.0c00633
ACS Synth. Biol. 2021, 10, 1640−1650

the batch of QC beads were used for the gain and detection threshold. For plasmid format UPR sensors, gating was applied to select the main population (>80% events). No gating was applied for chromosomally integrated UPR sensors, since the population fluorescence homogeneity was significantly more uniform than the respective plasmid forms (Figure S2).

Cellobiohydrolase I Activity Assay. The CBH activity assay was performed as described by Kroukamp et al. in 2017. In short, 25 μL of culture supernatant was mixed with 25 μL of 4 mM 4-methylumbelliferyl-*b*-D-lactoside (MULac; Carbosynth, Oxford, UK) in acetate buffer (pH 5.0). The reaction mix was incubated in Eppendorf tubes at 42 °C using a water bath for 30 min for Te.CBH and 4 h for Tr.CBH. The enzymatic reactions were stopped by the addition of 50 μL of 1 M sodium carbonate, and 80 μL of the final reaction mixture was transferred to a clear-bottom black 96-well plate. Fluorescence was measured on a BioTek Synergy H1 plate reader using the fluorescence intensity setting with ex/em wavelengths at 305/420 nm. To calculate the enzyme activity from the detected fluorescence values, a standard curve of ranging between 0.63 and 20.0 μM 4-methylumbelliferone was used. Enzymatic activity determinations were done in biological quadruplicates.

Mass Spectrometry. The supernatant was collected from relevant yeast culture, concentrated using a Pierce Protein Concentrator PES, at 30 kDa molecular weight cutoff, and then deglycosylated using PNGase F (NEB) followed by chloroform−methanol protein extraction. The dry samples were reconstituted with 50 μL of digestion buffer (6 M urea, 2 M thiourea, 100 mM HEPES buffer, pH 7.5) and then reduced with dithiothreitol and alkylated with iodoacetamide diluted with 25 mM NH_4HCO_3; then, after the addition of 0.8 μg of porcine trypsin, they were incubated overnight at 37 °C. Peptides were concentrated and desalted using C18 Zip-Tips (Millipore, Bedford, MA) as per the manufacturer's instructions. Peptides were resuspended in 50 μl of 3% (v/v) acetonitrile/0.1% (v/v) formic acid, briefly sonicated, and centrifuged at 16 000*g* for 5 min. Samples were separated by nano-LC using an Ultimate 3000 HPLC and autosampler system (Dionex, Amsterdam, Netherlands) coupled to an in-house built fritless nano 75 μm × 30 cm column packed with a ReproSil Pur 120 C18 stationary phase (1.9 μm, Dr, Maisch GmbH). LC mobile phase buffers were composed of A, 0.1% (v/v) formic acid, and B, 80% (v/v) acetonitrile/0.1% (v/v) formic acid. Peptides were eluted using a linear gradient of 5% B to 40% B over 60 min and then 95% B wash over 1 min at a flow rate of 250 nL/min. The LC was coupled to a QExactive Plus Orbitrap mass spectrometer (Thermo Fisher Scientific, Scoresby). The column voltage was 2300 V, and the heated capillary was set to 275 °C. Positive ions were generated by electrospray and the Orbitrap operated in data-dependent acquisition mode. A survey scan of 350−1550 m/z was acquired (resolution = 70 000, with an accumulation target value of 1 000 000 ions) with lockmass enabled. Up to 10 of the most abundant ions (>1.7e5 ions), with charge states ≥ +3, were sequentially isolated and fragmented, and a target value of 100 000 ions was collected. Ions selected for MS/MS were dynamically excluded for 20 s. The data were analyzed using Proteome Discoverer vr 2.4 (Thermo) and Mascot vr 2.7 (Matrix Science, London, UK). The search parameters included the following variable modifications: acetylation (protein N-terminal), oxidized methionine, and deamination (NQ), carbamidomethyl (C) and trypsin enzyme, and 10 ppm precursor mass tolerance. The databases were *Saccharomyces cerevisiae* (Uniprot) and an in-house "contaminants" database, which included the recombinant derived proteins. The results were filtered at a 1% FRD and keratin, with BSA and trypsin identifications excluded.

■ ASSOCIATED CONTENT

Supporting Information

The Supporting Information is available free of charge at https://pubs.acs.org/doi/10.1021/acssynbio.0c00633.

Tables of predicted UPREs of the native UPR promoters evaluated, nucleotide sequence of the synthetic minimal and hybrid UPR promoters, plasmids used in this study, and primers used in this study and figures of response of UPR sensors P-ERO1 and P-HAC1, fluorescence signal of the SM1 sensor as plasmid form P-SM1 and chromosomally integrated form G-SM1, and MS spectra (PDF)

■ AUTHOR INFORMATION

Corresponding Author

Heinrich Kroukamp − *ARC Centre of Excellence in Synthetic Biology, Department of Molecular Sciences and Biomolecular Discovery and Design Research Centre, Macquarie University, Sydney, NSW 2109, Australia;* orcid.org/0000-0002-9141-3112; Phone: +61 2 9850 8152; Email: heinrich.kroukamp@mq.edu.au

Authors

Kai Peng − *ARC Centre of Excellence in Synthetic Biology, Department of Molecular Sciences, Macquarie University, Sydney, NSW 2109, Australia*

Isak S. Pretorius − *Chancellery, Macquarie University, Sydney, NSW 2109, Australia*

Ian T. Paulsen − *ARC Centre of Excellence in Synthetic Biology, Department of Molecular Sciences and Biomolecular Discovery and Design Research Centre, Macquarie University, Sydney, NSW 2109, Australia*

Complete contact information is available at: https://pubs.acs.org/10.1021/acssynbio.0c00633

Author Contributions

‖K.P. and H.K. contributed equally. K.P. and H.K. conceived research project. H.K., K.P., I.T.P., and I.S.P. participated in the design, support, and coordination of the project. K.P. conducted the experiments. H.K. and K.P. analyzed data and wrote the manuscript. All authors read and approved the final manuscript.

Funding

This project was funded by the Biomolecular Discovery and Design Research Centre, Macquarie University, Sydney, Australia and the Centre of Excellence in Synthetic Biology funded by the Australian Government thorough its agency, the Australian Research Council. Infrastructure resources, in part, were provided by Bioplatforms Australia, Sydney.

Notes

The authors declare no competing financial interest.

■ ACKNOWLEDGMENTS

The authors would like to thank the Macquarie University and the Australian Research Council for funding this project through their respective research centres. The authors would

like to thank Dr. Ben Crossett and Angela Connolly for the mass spectrometry analysis that was carried out at Sydney Mass Spectrometry, a core research facility at the University of Sydney. The authors would also like to thank Russel Vincent at Macquarie University for discussion about the mass spectrometry.

■ ABBREVIATIONS

UPR, unfolded protein response; UPRE, unfolded protein response element; CBH, cellobiohydrolase; Tm, Tunicamycin; AFU, absolute fluorescence units

■ REFERENCES

(1) Mori, K. (2009) Signalling pathways in the unfolded protein response: development from yeast to mammals. *J. Biochem. 146*, 743−750.
(2) Walter, P., and Ron, D. (2011) The unfolded protein response: from stress pathway to homeostatic regulation. *Science 334*, 1081−1086.
(3) Promlek, T., Ishiwata-Kimata, Y., Shido, M., Sakuramoto, M., Kohno, K., and Kimata, Y. (2011) Membrane aberrancy and unfolded proteins activate the endoplasmic reticulum stress sensor Ire1 in different ways. *Mol. Biol. Cell 22*, 3520−3532.
(4) Volmer, R., van der Ploeg, K., and Ron, D. (2013) Membrane lipid saturation activates endoplasmic reticulum unfolded protein response transducers through their transmembrane domains. *Proc. Natl. Acad. Sci. U. S. A. 110*, 4628−4633.
(5) Volmer, R., and Ron, D. (2015) Lipid-dependent regulation of the unfolded protein response. *Curr. Opin. Cell Biol. 33*, 67−73.
(6) Kimata, Y., Ishiwata-Kimata, Y., Yamada, S., and Kohno, K. (2006) Yeast unfolded protein response pathway regulates expression of genes for anti-oxidative stress and for cell surface proteins. *Genes Cells 11*, 59−69.
(7) Bernales, S., McDonald, K. L., and Walter, P. (2006) Autophagy counterbalances endoplasmic reticulum expansion during the unfolded protein response. *PLoS Biol. 4*, e423.
(8) Travers, K., Patil, C., Wodicka, L., Lockhart, D., Weissman, J., and Walter, P. (2000) Functional and Genomic Analyses Reveal an Essential Coordination between the Unfolded Protein Response and ER-Associated Degradation. *Cell 101*, 249−258.
(9) Ng, D. T., Spear, E. D., and Walter, P. (2000) The unfolded protein response regulates multiple aspects of secretory and membrane protein biogenesis and endoplasmic reticulum quality control. *J. Cell Biol. 150*, 77−88.
(10) Hou, J., Tyo, K., Liu, Z., Petranovic, D., and Nielsen, J. (2012) Metabolic engineering of recombinant protein secretion by Saccharomyces cerevisiae. *FEMS Yeast Res. 12*, 491−510.
(11) Lin, J., Li, H., Yasumura, D., Cohen, H., Zhang, C., Panning, B., Shokat, K., LaVail, M., and Walter, P. (2007) *IRE1* Signaling Affects Cell Fate During the Unfolded Protein Response. *Science 318*, 944−949.
(12) Ma, Y., and Hendershot, L. M. (2004) The role of the unfolded protein response in tumour development: friend or foe? *Nat. Rev. Cancer 4*, 966−977.
(13) Cox, J., and Walter, P. (1996) A Novel Mechanism for Regulating Activity of a Transcription Factor That Controls the Unfolded Protein Response. *Cell 87*, 391−404.
(14) Pincus, D., Chevalier, M. W., Aragon, T., van Anken, E., Vidal, S. E., El-Samad, H., and Walter, P. (2010) BiP binding to the ER-stress sensor Ire1 tunes the homeostatic behavior of the unfolded protein response. *PLoS Biol. 8*, e1000415.
(15) Gardner, B. M., and Walter, P. (2011) Unfolded Proteins Are Ire1-Activating Ligands That Directly Induce the Unfolded Protein Response. *Science 333*, 1891−1894.
(16) Korennykh, A., Egea, P., Korostelev, A., Finer-Moore, J., Zhang, C., Shokat, K., Stroud, R., and Walter, P. (2009) The unfolded protein response signals through high-order assembly of Ire1. *Nature 457*, 687−693.
(17) van Anken, E., Pincus, D., Coyle, S., Aragon, T., Osman, C., Lari, F., Gomez Puerta, S., Korennykh, A. V., and Walter, P. (2014) Specificity in endoplasmic reticulum-stress signaling in yeast entails a step-wise engagement of HAC1 mRNA to clusters of the stress sensor Ire1. *eLife 3*, e05031.
(18) Sidrauski, C., and Walter, P. (1997) The transmembrane kinase Ire1p is a site-specific endonuclease that initiates mRNA splicing in the unfolded protein response. *Cell 90*, 1031−1039.
(19) Mori, K., Sant, A., Kohno, K., Normington, K., Gething, M., and Sambrook, J. (1992) A 22 bp cis-acting element is necessary and sufficient for the induction of the yeast *KAR2* (*BiP*) gene by unfolded proteins. *EMBO J. 11*, 2583−2593.
(20) Mori, K., Ogawa, N., Kawahara, T., Yanagi, H., and Yura, T. (1998) Palindrome with spacer of one nucleotide is characteristic of the cis-acting unfolded protein response element in *Saccharomyces cerevisiae*. *J. Biol. Chem. 273*, 9912−9920.
(21) Fordyce, P. M., Pincus, D., Kimmig, P., Nelson, C. S., El-Samad, H., Walter, P., and DeRisi, J. L. (2012) Basic leucine zipper transcription factor Hac1 binds DNA in two distinct modes as revealed by microfluidic analyses. *Proc. Natl. Acad. Sci. U. S. A. 109*, E3084−E3093.
(22) Gasser, B., Saloheimo, M., Rinas, U., Dragosits, M., Rodriguez-Carmona, E., Baumann, K., Giuliani, M., Parrilli, E., Branduardi, P., Lang, C., Porro, D., Ferrer, P., Tutino, M. L., Mattanovich, D., and Villaverde, A. (2008) Protein folding and conformational stress in microbial cells producing recombinant proteins: a host comparative overview. *Microb. Cell Fact. 7*, 11.
(23) Rahmat, E., and Kang, Y. (2020) Yeast metabolic engineering for the production of pharmaceutically important secondary metabolites. *Appl. Microbiol. Biotechnol. 104*, 4659−4674.
(24) Navarro-Tapia, E., Perez-Torrado, R., and Querol, A. (2017) Ethanol Effects Involve Non-canonical Unfolded Protein Response Activation in Yeast Cells. *Front. Microbiol. 8*, 383.
(25) Le, Q. G., Ishiwata-Kimata, Y., Kohno, K., and Kimata, Y. (2016) Cadmium impairs protein folding in the endoplasmic reticulum and induces the unfolded protein response. *FEMS Yeast Res. 16*, fow049.
(26) Patil, C., Li, H., and Walter, P. (2004) Gcn4p and Novel Upstream Activating Sequences Regulate Targets of the Unfolded Protein Response. *PLoS Biol. 2*, e246.
(27) Merksamer, P. I., Trusina, A., and Papa, F. R. (2008) Real-time redox measurements during endoplasmic reticulum stress reveal interlinked protein folding functions. *Cell 135*, 933−947.
(28) Xu, P., Raden, D., Doyle, F., and Robinson, A. (2005) Analysis of unfolded protein response during single-chain antibody expression in *Saccharomyces cerevisiae* reveals different roles for BiP and PDI in folding. *Metab. Eng. 7*, 269−279.
(29) Lajoie, P., Moir, R. D., Willis, I. M., and Snapp, E. L. (2012) Kar2p availability defines distinct forms of endoplasmic reticulum stress in living cells. *Mol. Biol. Cell 23*, 955−964.
(30) Aragon, T., van Anken, E., Pincus, D., Serafimova, I. M., Korennykh, A. V., Rubio, C. A., and Walter, P. (2009) Messenger RNA targeting to endoplasmic reticulum stress signalling sites. *Nature 457*, 736−740.
(31) Cedras, G., Kroukamp, H., Van Zyl, W. H., and Den Haan, R. (2020) The in vivo detection and measurement of the unfolded protein response in recombinant cellulase producing Saccharomyces cerevisiae strains. *Biotechnol. Appl. Biochem. 67*, 82−94.
(32) Pincus, D., Aranda-Diaz, A., Zuleta, I. A., Walter, P., and El-Samad, H. (2014) Delayed Ras/PKA signaling augments the unfolded protein response. *Proc. Natl. Acad. Sci. U. S. A. 111*, 14800−14805.
(33) Redden, H., and Alper, H. S. (2015) The development and characterization of synthetic minimal yeast promoters. *Nat. Commun. 6*, 7810.
(34) de Ruijter, J. C., Koskela, E. V., Nandania, J., Frey, A. D., and Velagapudi, V. (2018) Understanding the metabolic burden of

https://doi.org/10.1021/acssynbio.0c00633
ACS Synth. Biol. 2021, 10, 1640−1650

recombinant antibody production in *Saccharomyces cerevisiae* using a quantitative metabolomics approach. *Yeast 35*, 331−341.
(35) Ilmén, M., den Haan, R., Brevnova, E., McBride, J., Wiswall, E., Froehlich, A., Koivula, A., Voutilainen, S., Siika-aho, M., la Grange, D., Thorngren, N., Ahlgren, S., Mellon, M., Deleault, K., Rajgarhia, V., van Zyl, W., and Penttilä, M. (2011) High level secretion of cellobiohydrolases by Saccharomyces cerevisiae. *Biotechnol. Biofuels 4*, 30.
(36) Finger, A., Knop, M., and Wolf, D. H. (1993) Analysis of two mutated vacuolar proteins reveals a degradation pathway in the endoplasmic reticulum or a related compartment of yeast. *Eur. J. Biochem. 218*, 565−574.
(37) Gorgens, J. F., van Zyl, W. H., Knoetze, J. H., and Hahn-Hagerdal, B. (2001) The metabolic burden of the PGK1 and ADH2 promoter systems for heterologous xylanase production by Saccharomyces cerevisiae in defined medium. *Biotechnol. Bioeng. 73*, 238−245.
(38) Kroukamp, H., den Haan, R., la Grange, D. C., Sibanda, N., Foulquié-Moreno, M. R., Thevelein, J. M., and van Zyl, W. H. (2017) Strain breeding enhanced heterologous cellobiohydrolase secretion by Saccharomyces cerevisiae in a protein specific manner. *Biotechnol. J. 12*, 1700346.
(39) Valkonen, M., Penttilä, M., and Saloheimo, M. (2003) Effects of Inactivation and Constitutive Expression of the Unfolded- Protein Response Pathway on Protein Production in the Yeast Saccharomyces cerevisiae. *Appl. Environ. Microbiol. 69*, 2065−2072.
(40) Kroukamp, H., den Haan, R., van Zyl, J.-H., and van Zyl, W. H. (2018) Rational strain engineering interventions to enhance cellulase secretion by *Saccharomyces cerevisiae*. *Biofuels, Bioprod. Biorefin. 12*, 108−124.
(41) Kroukamp, H., den Haan, R., van Wyk, N., and van Zyl, W. H. (2013) Overexpression of native PSE1 and SOD1 in Saccharomyces cerevisiae improved heterologous cellulase secretion. *Appl. Energy 102*, 150−156.
(42) Gietz, R. D., and Schiestl, R. H. (2007) High-efficiency yeast transformation using the LiAc/SS carrier DNA/PEG method. *Nat. Protoc. 2*, 31−34.
(43) van Dijken, J. P., Bauer, J., Brambilla, L., Duboc, P., Francois, J. M., Gancedo, C., Giuseppin, M. L., Heijnen, J. J., Hoare, M., Lange, H. C., Madden, E. A., Niederberger, P., Nielsen, J., Parrou, J. L., Petit, T., Porro, D., Reuss, M., van Riel, N., Rizzi, M., Steensma, H. Y., Verrips, C. T., Vindelov, J., and Pronk, J. T. (2000) An interlaboratory comparison of physiological and genetic properties of four Saccharomyces cerevisiae strains. *Enzyme Microb. Technol. 26*, 706−714.
(44) Brachmann, C. B., Davies, A., Cost, G. J., Caputo, E., Li, J., Hieter, P., and Boeke, J. D. (1998) Designer deletion strains derived from Saccharomyces cerevisiae S288C: a useful set of strains and plasmids for PCR-mediated gene disruption and other applications. *Yeast 14*, 115−132.

https://doi.org/10.1021/acssynbio.0c00633
ACS Synth. Biol. 2021, 10, 1640−1650